Elsevier Editorial System(tm) for Journal of Marine Systems
Manuscript Draft

Manuscript Number:

Title: Increased frequency of wintertime stratification collapse events in the Gulf of Finland since 1990s

Article Type: Special Issue:BSSC-2011

Keywords: estuary; current straining; wind mixing work; destratification; wind regime change; Baltic Sea; Gulf of Finland

Corresponding Author: Prof. Jüri Elken, PhD

Corresponding Author's Institution: Marine Systems Institute at Tallinn University of Technology

First Author: Jüri Elken, PhD

Order of Authors: Jüri Elken, PhD; Urmas Raudsepp, PhD; Jaan Laanemets, PhD; Jelena Passenko; Ilja Maljutenko; Ove Pärn, PhD; Sirje Keevallik, PhD

Abstract: Since 1990s increased frequency of stratification collapse events in the Gulf of Finland has been noticed, when density difference between near-bottom and surface waters fell below 0.5 kg m 3. Such stratification crashes occur in winter months, from October-November to March-April when saline and thermal stratification decrease compared to the summer period according to the well-known seasonal cycle. The stratification decay process is forced primarily by the (1) westerly-southwesterly wind stress, causing anti-estuarine straining, and (2) direct wind mixing proportional to the wind speed cubed. The potential energy anomaly is occasionally reduced from the average winter level 70 J m 3 nearly to zero, manifesting the stratification collapse, when the work by current straining and the wind mixing work exceed significantly their average levels. Increased collapse frequency is caused by the shift of wind forcing. Namely, the average bimonthly cumulative westerly-southwesterly wind stress in December and January has increased from 1.7 N m-2 d during 1962-1988 to 3.7 N m-2 d during 1989-2007. The bimonthly wind mixing work per unit surface area has also increased from 7.5 kJ m-2 to 12.1 kJ m-2 from 1999 onwards.

Increased frequency of wintertime stratification collapse events in the Gulf of Finland since 1990s

Jüri Elken[a*], Urmas Raudsepp[a], Jaan Laanemets[a], Jelena Passenko[a], Ilja Maljutenko[a], Ove Pärn[a], Sirje Keevallik[a]

[a] Marine Systems Institute at Tallinn University of Technology, Akadeemia 15a, EE12618 Tallinn, Estonia

[*] Corresponding author, e-mail: elken@phys.sea.ee

Abstract

Since 1990s increased frequency of stratification collapse events in the Gulf of Finland has been noticed, when density difference between near-bottom and surface waters fell below 0.5 kg m^{-3}. Such stratification crashes occur in winter months, from October-November to March-April when saline and thermal stratification decrease compared to the summer period according to the well-known seasonal cycle. The stratification decay process is forced primarily by the (1) westerly-southwesterly wind stress, causing anti-estuarine straining, and (2) direct wind mixing proportional to the wind speed cubed. The potential energy anomaly is occasionally reduced from the average winter level 70 J m^{-3} nearly to zero, manifesting the stratification collapse, when the work by current straining and the wind mixing work exceed significantly their average levels. Increased collapse frequency is caused by the shift of wind forcing. Namely, the average bimonthly cumulative westerly-southwesterly wind stress in December and January has increased from 1.7 N m^{-2} d during 1962-1988 to 3.7 N m^{-2} d during 1989-2007. The bimonthly wind mixing work per unit surface area has also increased from 7.5 kJ m^{-2} to 12.1 kJ m^{-2} from 1999 onwards.

Keywords: estuary; current straining; wind mixing work; destratification; wind regime change; Baltic Sea; Gulf of Finland.

Highlights:

- During winter, the stratification is occasionally collapsed and well-mixed state occurs in the Gulf of Finland, an estuarine basin of the Baltic Sea.
- Potential energy anomaly of the water column is reduced by anti-estuarine current straining due to westerly-southwesterly winds and wind mixing work.
- Since 1990s, the work by wind in reducing the potential energy anomaly has increased, explaining the increased frequency of stratification collapse events.

1. Introduction

Kullenberg (1981) has noted, among others, that the Gulf of Finland (Fig. 1) is a "true estuarine embayment" of the Baltic Sea multi-basin brackishwater system. With its dimensions (about 400 km length, from 48 to 135 km width over most of the length), low salinity at the entrance (from 6–7 at the surface to 8–11 psu in the bottom layers below 80-100 m) and almost missing tides, the gulf is, however, quite unique among the world estuaries (Hansen and Rattray, 1966; see also the reviews by Alenius et al., 1998; MacCready and Geyer, 2010). The gulf has in the west a free 60-km wide and about 90-m deep connection to the Baltic Proper, the central basin of the system that undergoes in its northern part large variations of the stratification (e.g. Matthäus, 1984; Elken et al., 2006). River discharge is concentrated in the eastern part of the gulf, where the Neva River drains at the estuary head on the average 2400 $m^3 s^{-1}$ of freshwater, about 2/3 of the whole freshwater import to the gulf. Despite the large dimensions, compared to the internal Rossby radius (typical scales from 2 to 4 km, Alenius et al., 2003) and variable cyclonic circulation with a number of loops, eddies, fronts and upwelling events (Pavelson et al., 1997; Lehmann et al., 2002; Andrejev et al., 2004; Zhurbas et al., 2008; Lips et al., 2009, Elken et al., 2011), the along-basin salinity and density gradients are still well profound, especially when studied on the basis of temporally mean values over the seasons.

Salinity and stratification of the Gulf of Finland undergo strong seasonal variations (Haapala and Alenius, 1994). To the period of highest thermal stratification in summer, after the spring maximum of freshwater discharge, the surface salinity is decreased from the winter values of about 6.5 psu down to about 5.5 psu in the central part of the gulf. At the same time, the deep salinity at around 90-m depth is increased from about 7.5 psu to about 10 psu. While decrease of surface salinity during and after the period of high river discharge is a common feature of most of the estuaries (e.g. van Aken, 2008; Kimbro et al., 2009; Hong et al., 2010), then simultaneous increase of deep salinity is quite unique. The latter can be partly explained by the seasonal conditions of the adjacent larger sea basin, the Northern Baltic Proper (*e.g.* Matthäus, 1984), where below 80 m the intra-annual salinity variations can exceed 1 psu and the lowest deep salinity is usually observed during the winter.

Interannual changes of the oceanographic conditions of the Gulf of Finland reflect the variations in the large-scale forcing factors. A specific feature of the Baltic Sea is an intermittent nature of the large inflows of highly saline water from the North Sea (MBI-s, Major Baltic Inflows after Matthäus and Franck, 1992). With stronger and shallower halocline in the Baltic Proper, more saline water can be transported to the Gulf of Finland, increasing the strength of stratification and the extent of "salt wedge". During the stagnation periods, when MBI-s are missing for many years, the deep waters below the halocline (depth about 60-80 m in the eastern Baltic Proper) may become anoxic due to the absence of lateral advection of oxygen-rich water. Following the MBI-s, anoxic bottoms will disappear, but the area of low-oxygen (hypoxic) bottoms will increase because the halocline is usually lifted up (Conley et al., 2009). For the longest stagnation period 1977–1993, Kahru et al. (2000) noted that "in contrast to the Baltic Proper, in the Gulf of Finland, the stagnation period resulted in increased oxygen levels through enhanced vertical mixing arising from decreased salinity and weaker vertical stratification". Laine et al. (2007) have identified on the basis of monitoring data 1965-2000 similar long-term tendencies: decrease in salinity and density stratification until the early 1990s and a slight increase afterwards. In the oxygen content, opposite trends took place. Vermaat and Bouwer (2009) have proposed that reduced ice extent during the recent period has favored vertical mixing, causing reduction of the extent of hypoxic bottoms.

Among the complex ventilation processes (Meier et al., 2006), convection due to surface cooling, turbulent erosion from surface towards deeper layers and turbulent shear mixing are usually considered as most important in the Gulf of Finland. During the summer, a significant decay of observed stratification has been explained by persistent south-westerly winds, creating a temporary estuarine circulation reversal (Elken et al., 2003). With reference to other estuaries, Blumberg and Goodrich (1990) showed for the Chesapeake Bay that wind-induced current shear is more effective in destratification than surface-generated turbulence. In the framework of estuarine dynamical concepts, Scully et al. (2005) also pointed to the role of wind-induced current straining, interacting with along-basin density gradients.

During the winter, the period of weakest stratification in the Gulf of Finland, the observational data are quite rare. Still, events of complete stratification collapse (reaching the well-mixed state) can be frequently observed during recent winters. These situations, when bottom to surface density difference (and consequently, potential energy anomaly) reduce drastically close to zero, cannot persist over longer times since longitudinal gradients of mean density restore the stratification.

The paper is aimed to study the stratification collapse events in the Gulf of Finland and to find the governing mechanisms for such events. Further on, we study, whether the collapse events likely occur also during non-sampled times. It is also interesting to know, if there is a change of frequency of complete destratification, related to the changing climate factors.

Our hypothesis is that purely vertical mixing processes in the Gulf of Finland are not always strong enough to make the complete destratification as observed, and wind-induced current straining is important. To evaluate the role of different mechanisms, we use the balance for vertically integrated potential energy anomaly (Simpson et al., 1990; Burchard and Hofmeister, 2008; Wang et al., 2011). The "normal" wintertime potential energy anomaly (PEA) values are determined from the hydrographic observations and they reflect the average forcing conditions. We study further PEA change due to current straining and direct wind mixing, using the data from long-term wind observations. Straining effect is estimated from the established correlation between the specific wind stress component and the time-dependent amplitude of the "strain" EOF mode of along-basin currents. The wind-to-EOF dependency is found from a numerical model. Effect of direct wind mixing is evaluated from the cubic relation to the wind speed. Changes of PEA are calculated for the ice-free periods of each winter. The paper ends with the discussion of the relation of PEA changes to the climatic forcing data.

2. Data and methods

2.1. Observational data

The basic data set is about stratification in the Gulf of Finland. We used long-term data of hydrographic observations 1900–2010 extracted from the ICES international database. The data are mainly from the standard depths (*e.g.* Haapala and Alenius, 1994; Janssen et al., 1999). Deeper layers have less data coverage than the surface, especially in the first half of the period. We focused on the data around HELCOM monitoring station BMP F3 (historically known also as LL7, φ = 59.8465°N, λ = 24.8378°E) with a 15 km radius. This station is located in the deepest part of the central area of the gulf near the transect Tallinn-Helsinki, with the depth range 80–110 m. The ICES data were complemented with 38 profiles from national CTD data set, observed since 1984. They were also converted to the standard depths, to keep homogeneity with historical data.

The main aim of the analysis was to characterize the strength of stratification over time, especially during the winter period. The basic approach is to investigate the near-bottom ρ_b to surface ρ_s density difference $\rho_b - \rho_s$, as can be found in many studies (*e.g.* Laine et al., 2007). For the deep values, we used the closest depth to 70 m below that value. In total we obtained 47 values of $\rho_b - \rho_s$ in December and January since 1975.

Strength of variable stratification can be more precisely (in terms of dynamic equations) characterized by the potential energy anomaly (PEA), the potential energy of the water column of a thickness H relative to the well-mixed state when the initial density ρ takes the depth-mean value

$$\bar{\rho} = \frac{1}{H}\int_{-H}^{0} \rho \, dz \ . \qquad (1)$$

Following the definitions, *e.g.* by Simpson (1981) and Simpson et al. (1990), PEA per unit volume of the water column (J m^{-3}), as work needed to convert the water column into a well-mixed state, is

$$\varphi = \frac{g}{H}\int_{-H}^{0} (\bar{\rho} - \rho) z \, dz \ . \qquad (2)$$

PEA is zero for the well-mixed state and positive for stable stratification.

The main question in PEA calculation is to refer the data into fixed levels (compared to slightly variable levels in observational data). We used linear interpolation/extrapolation to the levels of 0 m and 70 m, when the depth difference with the sampled value did not exceed 5 m. Only profiles with at least 7 data points between 0 and 70 m were taken into account. Unfortunately, there were no data in 1915–1920 and 1940–1953 that could meet the above criteria.

For the evaluation of wind forcing we used the 3-hourly wind observations at Utö meteorological station provided by Finnish Meteorological Institute since 1961. The station is located on the island at the entrance to the Gulf of Finland (Fig. 1) and presents well the wind conditions over the open part of the Gulf of Finland (Soomere and Keevallik, 2003). In order to take into account variable ice conditions at wind forcing during the winter, we used digitized ice charts from the archive of Estonian Meteorological and Hydrological Institute (Pärn and Haapala, 2011).

2.2. Model data

We used the data from 10-years simulation 1997–2006 made by the General Estuarine Transport Model (GETM) described in detail by Burchard et al. (2004). The model setup used 25 sigma layers with horizontal resolution of the model grid 2 nautical miles for the whole Baltic Sea. The bathymetry has been interpolated on the computation grids from the digital topography by Seifert et al. (2001). Depths have been adjusted so that the maximum depth is 260 m. Initial temperature and salinity fields were constructed using the Data Assimilation System coupled with the Baltic Environmental Database at the Stockholm University (http://nest.su.se/das). Atmospheric forcing (wind stress and heat flux components) with 3-h intervals was adopted from ERA40 re-analysis data dynamically downscaled with the Rossby Centre Atmosphere Ocean model (Döscher et al., 2010). For sea level elevations at the open boundary in the northern Kattegat 1-hourly averaged measurements at Smøgen (Sweden) were used. Salinity and temperature at the open boundary have been adopted from the climatological mean fields by Janssen et al. (1999). The model output during the long-term run was written with 1 day interval, which is adequate for temperature and salinity but does not represent short-term current variations.

Variations of currents and sea level were investigated from the results by operational HIROMB model (*e.g.* Lagemaa et al., 2011). The finest grid of the setup by Swedish Meteorological and Hydrological Institute has a resolution of 1 nautical mile. Vertical fixed levels have layer thickness from 4 m near the surface to 15 m near 100-m depth. We used hourly output data for 2005–2009 to study the EOF modes of currents in relation to wind forcing.

3. Results and discussion

3.1. Observational evidence of temporary stratification collapse

Re-inspection of historical hydrographic time series in the Gulf of Finland has drawn our attention to the “missing stratification” profiles during the winter. We collected the profiles from December and January as shown in Fig. 2. On the background of normal (weaker than during the summer) stratification, several vertically nearly constant profiles can be identified. One can suspect the instrument failure during ice conditions. According to the database, such unusual profiles were carefully checked. For example in 14 January 2000, Finnish research vessel ARANDA made 3 consecutive profiles at station BMP F3, all exposing the same stratification collapse. Events of well-mixed state are occasionally observed during the winter, but they are not so easy to catch because of historically low sampling frequency.

We define the stratification collapse as an event when bottom-to-surface density difference becomes less than 0.5 kg m^{-3}. Time series of bottom-to-surface density difference, observed at station BMP F3 during December and January (Fig. 3) reveals 11 winters with collapse out of 26 winters when observations were available. We note again the poor data availability during the winter; several winters have no observations due to the hard navigation conditions during ice cover and/or winter storms. Also, collapse is a short-term event that may be not caught by irregular and sparse sampling.

In order to quantify the stratification collapse in terms of potential energy anomaly (PEA), we calculated the PEA values in a 15 km radius around the station BMP F3, based on hydrographic observations from 1901 onwards. In summer the PEA values are higher than during the winter, and the highest value 360 J m^{-3} was found during the summer 1930. The very high values, above 300 J m^{-3}, were also observed during the summers 1970, 1973, 1980, 1983, 1988, 1994 and 2004–2006. Compared to the beginning of the 20th century, the PEA variation range has slightly increased: Summer maximums increased from 280 to 350 J m^{-3} and winter minimums decreased from 20 J m^{-3} to nearly zero. Seasonal PEA cycle for the whole observational data set is presented in Fig. 4. The median PEA in winter is about 70 J m^{-3} but the variation range is from nearly zero to 160 J m^{-3}. The stratification collapse may be defined as the PEA value below 30 J m^{-3}. Such values were observed 44 times during the low stratification season from October to April, most frequently in January (13 times).

3.2. Evaluation of wind-induced current straining and direct mixing

We are further interested to evaluate the role of different dynamical factors in creating wintertime destratification and eventual stratification collapses. Here we consider the main assumptions of potential energy conversion.

Change of potential energy anomaly (PEA) is governed by the energy conversion budget (W m^{-3})

$$\frac{\partial \varphi}{\partial t} = \frac{\partial \varphi_S}{\partial t} + \frac{\partial \varphi_W}{\partial t} + \frac{\partial \varphi_Q}{\partial t} + D_\varphi, \qquad (3)$$

where the terms of our interest (further evaluated step by step) are: φ_S is the work done by current straining (vertically differential lateral advection on the background of mean estuarine gradients), φ_W denotes the work by direct vertical (wind) mixing, φ_Q is the work done by heating or cooling of the water surface and D_φ reflects the power of other processes in change of PEA. Complete derivation of (3) has been given by Burchard and Hofmeister (2008).

The power from current straining (work per unit time) can be estimated

$$\frac{\partial \varphi_S}{\partial t} = \frac{g}{H} \frac{\partial \bar{\rho}}{\partial x} \int_{-H}^{0} (u - \bar{u}) z \, dz, \qquad (4)$$

where

$$\bar{u} = \frac{1}{H} \int_{-H}^{0} u \, dz \qquad (5)$$

is the vertical mean (over depth H) of along-basin velocity u. Positive values of (4) mean strengthening of stratification.

In (4) we assume constant along-basin density gradient over the depth and time. Indeed, long-term mean $\frac{\partial \rho}{\partial x}$ is about $-4.5 \cdot 10^{-6}$ kg m^{-4} in the surface and deep layers by the results of climatic simulations using the GETM model, somewhat smaller gradients are found in the mid-depths.

The long-term mean of the vertically averaged current $\langle \bar{u} \rangle$ is due to the river discharge, distributed over the cross-section area of the basin. In the Gulf of Finland, taking the section area 3 km^2 (Elken et al., 2011) and mean river discharge 3600 m^3 s^{-1}, the depth-mean current is negligible - about 0.12 cm s^{-1}. On shorter time scales, variations of $\bar{u}$ are related to the basin volume changes due to fluctuating mean sea level changes. Within the time scales of weeks and months, the mean sea level of the Gulf of Finland may vary together with the overall Baltic sea level by about 0.5 m in 10 days (neglecting the short-term storm pulses and Baltic Sea seiches), yielding the variability range of $\bar{u}$ about 0.5 cm s^{-1} (the gulf surface area is about 29,500 km^2). Baroclinic currents have much higher speed range of 10–20 cm s^{-1} and their contribution to PEA evolving is of primary interest.

Further we want to estimate time series of (4) over a long period using only the wind data. Elken et al. (2011) have shown that along-basin currents can be decomposed on the cross-basin transects of the Gulf of Finland by the EOF analysis into a “flat” barotropic mode (unidirectional over the whole water column, 23%–42%, correlated with the short-term volume changes), a two-layer mode (surface Ekman transport with the deeper compensation flow, 19%–22%, correlated with the southwesterly wind stress component) and a number of other modes. While the 1st mode resembles an analogue to the tidal effects, then the 2nd mode can produce wind induced current straining. In order to evaluate the time- and depthdependent along-basin current component $u(z,t)$ in (4), we recalculate the EOF modes (Fig. 5) from the hourly HIROMB model data over two winter months from December 2005 to January 2009. For that purpose we take the initial data as cross-basin averages of $u-\bar{u}$ over the deeper part of the basin with depths more than 50 m, in order to exclude coastal currents. We use the decomposition

$$u(z_k,t_n)=\langle u\rangle_k+\sum_{m=1}^{M}A_m(t_n)\,F_m(z_k), \tag{6}$$

where $\langle u\rangle_k$ is the temporally mean vertical profile of current, $F_m(z_k)$ are dimensional EOF modes ($m=1\ldots M$ is the mode number, with M equal to the number of vertical data points K, $k=1\ldots K$) and $A_m(t_n)$ are non-dimensional amplitudes, to yield the unit standard deviation over the whole time period. We have calculated the EOF modes for two longitudinal sections, along 23.65°E (section A, at the gulf entrance) and 24.38°E (section B, near BMP F3). The amplitude of the 2nd mode $A_2(t_n)$ has quite good correlation with the southwesterly wind stress component at both of the sections. Namely, on section B the correlation squared R^2 is significantly above 0.5 for the wind directional range 190°–250° (positive slope, maximum R^2 = 0.60 for directions 210°–220°) and 10°–60° (negative slope) and the correlation is missing (below 0.1) for directions 290°–330° and 110°–150°. Amplitudes from section A are highly correlated with those from section B. The high-correlation regression is $A_m(t_n)=a_S\,c_D\,\rho_a\,W_{SW}(t_n)W(t_n)$, where a_S is the empirical slope (6.8 and 7.8 $m^2\ N^{-1}$ for the A and B, respectively), W_{SW} is the southwesterly wind speed component, W is scalar wind speed and ρ_a = 1.2 kg m^{-3} is the density of air and c_D =1.3·10^{-3} is drag coefficient. The value of integral in expression (4) over 90-m depth, using the 2nd EOF mode as shown in Fig. 6, is about 78 $m^3\ s^{-1}$ for both of the sections. Consequently, the estimate for power from wind straining per unit surface area is

$$\frac{\partial\Phi_S}{\partial t}=H\,\frac{\partial\varphi_S}{\partial t}=A_S\,g\,\frac{\partial\bar{\rho}}{\partial x}\,c_D\,\rho_a\,W_{SW}\,W\ . \tag{7}$$

The site-specific value of A_S has been estimated empirically from the HIROMB model results. We adopt A_S =570 m^4 s kg^{-1} since the individual values on sections A and B are 530 and 610 m^4 s kg^{-1}, respectively. Within this estimate, the southwesterly wind stress $\tau_{SW}=c_D\,\rho_a\,W_{SW}\,W$ of 0.1 N m^{-2} (wind speed about 8 m s^{-1}) creates anti-estuarine straining power of -2.5·10^{-3} W m^{-2}, *i.e.* weakening of stratification. Power from straining by $\langle u\rangle_k$ is only 0.4·10^{-3} W m^{-2} and we have omitted it in (7). During the EOF calculation period, the mean wind vector was from south-west with a speed 3.3 m s^{-1}, superimposed by isotropic wind vector variations with standard deviation 6.2 m s^{-1}. Therefore the mean eastward current at the surface as shown in Fig. 6 reflects the Ekman drift.

PEA is reduced by mixing through a chain of processes that depend on the wind (the term φ_W in (3)). Mixing power per unit surface area, generated by wind, can be estimated in cubic formulation from the wind speed W

$$\frac{\partial\Phi_W}{\partial t}=H\,\frac{\partial\varphi_W}{\partial t}=-\gamma\,c_D\rho_a\,W^3, \tag{8}$$

where $\gamma = 10^{-3}$ is non-dimensional mixing efficiency parameter (see the discussion by Pavelson et al., 1997). As an example of the range of values, for reducing the average winter PEA level 70 J m^{-3} of the 70-m layer to zero in a weekly stormy period, (constant) W must exceed 17 m s^{-1}.

Temperature lies during winter within a few °C around the temperature of maximum density. Therefore changing temperature has negligible effect on water density and the work done by heating or cooling of the water surface (φ_Q in (3)) may be omitted in the PEA balance.

At present stage of knowledge, the contribution of other processes (D_φ in (3)) is unknown in the Gulf of Finland. We use later the assumption that stratification restoring by D_φ is over the time average in balance with mean destratifying terms by straining and wind mixing.

The relations (7) and (8) can be interpreted using a specific case of two stratification situations given in Fig. 6 along the main axis of the gulf, simulated using the GETM model. From 27 November to 12 December 1999, after 15 days of strong southwesterly winds with speeds 10–15 m s^{-1} (according to the model forcing data), the salt wedge lying under the halocline was considerably pushed out from the gulf, the halocline got deeper and/or disappeared. As calculated from the modeled density distributions, PEA was reduced at section A (23.65°E) by about 120 J m^{-3} but remained unchanged at section B (24.38°E) and eastward from it. Average PEA reduction in the western half of the Gulf of Finland can be estimated 60 J m^{-3}, for the surface area of the whole water column it gives the estimate 5.4 kJ m^{-2}. The southwesterly wind impulse (cumulative wind stress) was 1.2 N m^{-2} d, giving according to (7) PEA reduction due to wind straining 2.6 kJ m^{-2}. Time integration of (8) gave PEA reduction due to direct wind mixing 2 kJ m^{-2}. The sum of these two estimated work amounts corresponds roughly to the calculated loss of PEA. From this example we learnt, that expressions (7) and (8) do not resolve the PEA change details in space and time, but they can be used for gross estimates of PEA reduction due to anti-estuarine wind straining and direct wind mixing. We also found, that in the particular model case the straining work slightly exceeded the wind mixing work.

3.3. Time series evaluation of wind effects on PEA

Based on the relations (7) and (8), we estimate contributions of wind-induced current straining and direct wind mixing in changing PEA during the winter months from December to January. Based on the hourly wind data observed at Utö meteorological station during 1961-2007, we have made time integrations of wind-dependent terms for each winter.

According to (7), cumulative westerly-southwesterly wind stress (wind impulse)

$$T_{SW} = \int_0^t \tau_{SW} dt = c_D \, \rho_a \int_0^t W_{SW} W dt \qquad (9)$$

of 1 N m^{-2} d creates PEA change $\Delta\Phi_S$ due to the work by straining by about 2 kJ m^{-2},

$$\Delta\Phi_S = A_S \, g \frac{\partial \bar{\rho}}{\partial x} T_{SW} \, . \qquad (10)$$

The wintertime bimonthly wind impulse time series (Fig. 7) reveal remarkable changes, from -2 to 8 N m^{-2} d. On the average, the westerly-southwesterly wind impulse $T_{SW}(t)$ is positive. Exceptions are the winters 1966 (year taken by January), 1967, 1977, 1979, 1982, 1985 and 1987 when northeasterly wind stress dominated over two-month period. Since the winter 1988, the wind impulses have been only positive, favoring anti-estuarine transport in the Gulf of Finland. Because $T_{SW}(t)$ is changing over time, we have also found maximum positive values of $T_{SW}(t)$ corresponding to maximum PEA reduction due to straining. From 1989 onwards, westerly-southwesterly winds have dominated throughout the winter and maximum $T_{SW}(t)$ values are found at the end of January.

Using the shift detection technique by Rodionov (2004), the mean bimonthly westerly-southwesterly wind impulse is about 1.7 N m^{-2} d during 1962-1988 and about 3.7 N m^{-2} d during 1989-2007. At the regime shift detection the cut-off length was set to 10 years and the Huber's weight parameter to 2. The latter means that the values exceeding two standard deviations from the regime are considered to be outliers and a certain weighing procedure is applied to them to estimate the average values of the regimes. In the present case, only one outlier was detected – in 1992. Setting the Huber's parameter to 1, the number of outliers increased to 12, but this procedure changed only the average values of the regimes and did not affect the switch-time of the shift. The chosen cut-off length of 10 years guarantees that the regimes that are longer will be detected, but detection of shorter regimes is not excluded.

Increase of mean bimonthly westerly-southwesterly wind impulse by 2 N m^{-2} d corresponds to the PEA reduction $-\Delta\Phi_S$ by about 4.4 kJ m^{-2} and potentially might cause full destratification of the water column, if stratification restoring factors and changes in mixing intensity are not taken into account. Note that the observed average wintertime PEA level 70–100 J m^{-3} per unit volume corresponds to 5–7 kJ m^{-2} per unit surface area of the 70-m water column.

PEA change due to direct wind mixing $\Delta\Phi_W$ is estimated by time integration of the relation (8)

$$\Delta\Phi_W = -\gamma\, c_D \rho_a \int_0^t W^3 dt\,. \qquad (11)$$

On the average, the wintertime bimonthly wind mixing work (Fig. 8) for PEA reduction $-\Delta\Phi_W$ is frequently 5–7 kJ m^{-2} but can exceed 15 kJ m^{-2} as observed in 2000 and 2005. Higher $-\Delta\Phi_W$ values were observed also in the winters of 1965, 1993, 2004 and 2007. The applied regime shift detection technique revealed that the mean value about 7.5 kJ m^{-2}, evident for 1962–1998, increased to 12.1 kJ m^{-2} from 1999 onwards. However, this regime shift is less reliable than the change observed in the westerly-southwesterly wind stress.

Effects of ice cover on wind mixing and currents are not well known, since they depend on the ice concentration, ice types, vicinity of coasts etc. Zhang and Lepparanta (1995) have noted that in ice conditions water piling-up is decreased and sea level slope, forcing the deep currents, may be reduced to 1/3 of the value of ice-free slope in similar wind conditions. For the rough calculation, we assumed that free atmosphere-to-sea transfer occurs if less than 50% of the western Gulf of Finland is covered by ice, and blocking occurs at more extensive ice cover. The results, given in Figs. 7 and 8 show that high values of $-\Delta\Phi_S$ and $-\Delta\Phi_W$ occur in mild winters when the surface waters of the western gulf are nearly ice-free until the end of January. During severe winters, the PEA reduction by straining $-\Delta\Phi_S$ was as a rule much lower than the average value of the period.

For the independent interpretation, the PEA time series calculated from the GETM model results for 1997–2006 showed minimum values during the winter. Average PEA level per unit area was 5–7 kJ m^{-2}, well in the range of observed values, but remarkable changes occurred, from 1 to 19 kJ m^{-2}. Strongest stratification, with highest PEA was modeled for the 2003 severe winter with early ice cover. Low PEA values were modeled for the winters 1999, 2000 and 2005. While the first winter was not sampled, for the two latter cases the stratification collapse was observationally also caught, since by the model data the low PEA periods were quite long, several tens of days.

For full mixing of the water column, additional work by 5–7 kJ m^{-2} is needed to change the "normal" situation. We assume that in the long-term average conditions, the $\langle -\Delta\Phi_S \rangle$ value about 6 kJ m^{-2} and $\langle -\Delta\Phi_W \rangle$ value about 8 kJ m^{-2} are balanced by PEA production due to the average freshwater discharge and average higher salinity/density of the inflowing open sea waters. For the collapse forcing criterion, we need to find the value $\Delta\Phi_{cr}$ which exceeding $-\Delta\Phi_S - \Delta\Phi_w > \Delta\Phi_{cr}$ creates the event. Best match with the observed cases was found for $\Delta\Phi_{cr}$ =14 kJ m^{-2}. Among the wintertime stratification observations in 23 winters during December and January, all the collapse cases satisfied this criterion, except for the winter 1978. Therefore we consider that our approach to assess the stratification collapses based only on the wind data is workable.

Based on the episodic time series of wintertime stratification observations (Fig. 3), we have very rough collapse frequency estimation: during 1975–1989 from 9 winters with available measurements, stratification collapse was evident during 3 winters, collapse frequency 1/3; in 1990-2008 we found 14 observed winters, whereas collapse was evident in 7 winters, frequency 1/2. Within these low sample amounts, the frequency estimation is, however, quite voluntary. Confidence of determination is increased by inclusion of estimates of potential energy conversion from regular wind observations, presented above: we estimate an increase of wintertime collapse frequency from 40% to 60%.

3.4. Further interpretation and outlook

Although increased mixing in the Gulf of Finland has been briefly noted in several papers and data reports, the events of temporary stratification collapse have not got attention so far. The reasons for such ignorance could be (a) difficult wintertime sampling logistics due to ice cover and/or winter storms, and (b) problems of validating the numerical models in reproducing the short-term stratification events (except for upwelling, that is modeled adequately).

We have extended the knowledge from limited historical observations to the PEA changes, using the relations to the wind forcing. One of the key findings is the approximate relation of PEA reduction to the impulse (cumulative wind stress) of westerly-southwesterly winds. This approach, derived from the EOF analysis of vertical current profiles and correlative relation of the "straining" EOF mode amplitude to the wind stress projection, is in agreement with earlier findings by Krauss and Brügge (1991).They obtained that the transport through the Stolpe Channel is proportional to the wind stress projected to a specific (not necessarily along-channel) direction. For the Gulf of Finland, importance of southwesterly wind on the forcing of along-basin transport was presented by Elken et al. (2003). While the deep transport is geostrophically related to the cross-basin sea level slope, the slope relation to the forcing wind stress remained empirical. In the present study we also had to use the site-specific constants in relation (7). Feng and Li (2010) have found that in the estuary with an open mouth, both wind components cause nearly equal sea level changes. Their model is an extension of that by Garvine (1985). Forcing of sea level slopes in an elongated estuary has been also considered by Reyes-Hernandez and Valle-Levinson (2010) and Hinata et al. (2010). These results partly explain the found empirical wind direction relationship and also motivate further studies of wind-forced motions in the Baltic Sea.

Considering the wintertime impulse of westerly-southwesterly winds, our analysis shows that a shift has taken place in 1989. The chosen cut-off length of 10 years guarantees that the regimes that are longer will be detected. The observed shift in wind regime supports the increase of temporary reversals of estuarine circulation in the Gulf of Finland. Such a change is caused by the larger scale climatic processes. Meier (2005) has found that recent decrease of the average salinity of the Baltic is caused by the increase of zonal winds. It is widely recognized that the western flow over North-East Europe has intensified during winter months. Keevallik (2011) has shown that this intensification can partly be ascribed to an abrupt increase in the upper-air zonal wind component in January and February around 1987. Such an increase is accompanied by a shift in the meteorological regime at the surface: During the period of 1987-1989 simultaneous shifts have taken place at the observation sites in Estonia where the monthly mean zonal wind component, temperature and precipitation have increased. Such findings are supported by other investigations that also suggest switch-like changes in meteorological regime at the end of the 1980s (Lehmann et al. 2011, Kyselý and Domonkos 2006).

The results in the present paper are based on the routine hydrography and wind observations and unfortunately lack any details of spatio-temporal features of stratification collapse events. Therefore several detailed studies of wintertime dynamics are just started or are in a planning phase. It is of significant interest to consider also ecological effects of abrupt stratification dynamics. During strong stratification, hypoxic conditions may develop near the bottom (Kahru et al., 2000; Laine et al., 2007; Conley et al., 2009), favoring release of accumulated phosphorus from the sediments. But how, by which processes, the new near-bottom phosphorus is transported to the euphotic layer when the stratification is strong? Eventual collapse of stratification is likely one important process to bring the (before collapse) bottom-released nutrients back into the active ecological cycle and to intensify eutrophication and harmful algal blooms. On the other hand, if mixing throughout the water column is intensive, hypoxia does not develop and benthic communities have favorable living conditions. We hypothesize that climatic change of the dominance of the two stratification collapse processes – wind-direction-dependent current straining and direction-independent direct wind mixing – might have different consequences for the marine ecosystem health in the Gulf of Finland: the first one amplifying the eutrophication and the second one improving the living conditions for the benthic communities.

4. Conclusions

A measure of the stratification strength - potential energy anomaly (PEA) - has in the central and western parts of the Gulf of Finland average wintertime value per unit surface area about 5 kJ m^{-2} for the depth range of 70-80 m. This PEA level is balanced by the PEA production due to the freshwater discharge and inflow of open sea waters of higher salinity and density, and PEA reduction. The PEA is occasionally reduced nearly to zero, manifesting the stratification collapse, when the wind mixing work and the work by current straining due to southwesterly winds exceed significantly their average levels. In the bimonthly scale, in December and January, the estimates for average work by current straining and wind mixing are 6 and 8 kJ m^{-2}, respectively. These estimates are based on the observed time series of wind and the derived relations for PEA change. The relations are validated by the results from episodic hydrographic observations. During all the observed stratification collapse cases, the wind-dependent PEA reduction work, with reference to the long-term average work, exceeded the average PEA level. Since 1991, “overshoot” of PEA reduction compared to its average level increased, implying longer duration of collapse events.

Analysis of wind data, using the derived and validated PEA relations, showed that since 1990s there has been increased frequency of stratification collapse events and increased duration of such events. This change is most probably related to an abrupt increase in the upper-air zonal wind component around 1987 in January and February over North-East Europe that may form a significant part of the intensification of the western flow. As a result, since the late 1980s the winter season of the Baltic Sea area tends to be warmer, with less ice cover and warmer sea surface temperature. In Estonia, near the Gulf of Finland, abrupt increase in the monthly mean zonal wind component and temperature has taken place in January and February.

Acknowledgments

The present study was initiated by finding and interpretation of the “missing stratification” profiles, re-inspected in the course of preparing the model validation data set within the BONUS+ ECOSUPPORT project. The study was supported by the Estonian Science Foundation grants No 7328 and 7467; the results were also used in writing of the proposals of the grants No 9278 and 9382.

References

Alenius, P., Myrberg, K., Nekrasov, A., 1998. The physical oceanography of the Gulf of Finland: a review. Boreal Environment Research 3, 97–125.

Alenius, P., Nekrasov, A., Myrberg, K., 2003. Variability of the baroclinic Rossby radius in the Gulf of Finland. Continental Shelf Research 23, 563–573.

Andrejev, O., Myrberg, K., Alenius, P., Lundberg, P.A., 2004. Mean circulation and water exchange in the Gulf of Finland - a study based on three-dimensional modelling. Boreal Environment Research 9, 9–16.

Blumberg, A.F., Goodrich, D.M., 1990. Modeling of wind-induced destratification in Chesapeake Bay. Estuaries 13 (3), 236–249.

Burchard, H., Bolding, K., Villarreal, M.R., 2004. Three-dimensional modelling of estuarine turbidity maxima in a tidal estuary. Ocean Dynamics 54, 250–265.

Burchard, H., Hofmeister, R., 2008. A dynamic equation for the potential energy anomaly for analysing mixing and stratification in estuaries and coastal seas. Estuarine, Coastal and Shelf Science 77, 679–687.

Conley, D.J., Björck, S., Bonsdorff, E., et al. 2009. Hypoxia-Related Processes in the Baltic Sea. Environmental Science & Technology 43, 3412–3420.

Döscher, R., 2010. Wyser, K., Meier, H.E.M., Qian, M., Redler, R., 2010. Quantifying Arctic contributions to climate predictability in a regional coupled ocean-ice-atmosphere model. Climate Dynamics 34, 1157–1176.

Elken, J., Mälkki, P., Alenius, P., Stipa, T.,2006. Large halocline variations in the Northern Baltic Proper and associated meso- and basin-scale processes. Oceanologia 48(S), 91–117.

Elken, J., Nõmm, M., Lagemaa, P., 2011. Circulation patterns in the Gulf of Finland derived from the EOF analysis of model results. Boreal Environment Research 16A, 84–102.

Elken, J., Raudsepp, U., Lips, U., 2003. On the estuarine transport reversal in deep layers of the Gulf of Finland. Journal of Sea Research 49, 267–274.

Feng, Z., Li, C., 2010. Cold-front-induced flushing of the Louisiana Bays. Journal of Marine Systems 82, 252–264.
Garvine, R.W., 1985. A simple model of estuarine subtidal fluctuations forced by local and remote wind stress. Journal of Geophysical Research 90 (C6), 11945–11948.
Haapala, J., Alenius, P., 1994. Temperature and salinity statistics for the Northern Baltic Sea 1961–1990. Finnish Marine Research 262, 51–121.
Hansen, D.V., Rattray, M., 1966. New dimensions in estuary classification. Limnology and Oceanography 11(3), 319–326.
Hinata, H., Kanatsu, N., Fujii, S., 2010. Dependence of Wind-Driven Current on Wind Stress Direction in a Small Semienclosed, Homogeneous Rotating Basin. Journal of Physical Oceanography 40, 1488–1500.
Hong, B., Panday, N., Shen, J., Wang, H.V., Gong, W., Soehl, A., 2010. Modeling water exchange between Baltimore Harbor and Chesapeake Bay using artificial tracers: seasonal variations. Marine Environmental Research doi: 10.1016/j.marenvres.2010.03.010
Janssen, F., Schrum, C., Backhaus, J., 1999. A climatological data set of temperature and salinity for the North Sea and the Baltic Sea. Deutsche Hydrographische Zeitung, Suppl 9.
Kahru, M., Leppänen, J.M., Rud, O., Savchuk, O.P., 2000. Cyanobacteria blooms in the Gulf of Finland triggered by saltwater inflow into the Baltic Sea. Marine Ecology Progress Series 207, 13–18.
Keevallik, S., 2011. Shifts in meteorological regime of the late winter and early spring in Estonia during recent decades. Theoretical and Applied Climatology 105 (1-2), 209-215
Kimbro, D.L., Largier, J., Grosholz, E.D., 2009. Coastal oceanographic processes influence the growth and size of a key estuarine species, the Olympia oyster. Limnology and Oceanography 54 (5), 1425–1437.
Krauss, W., Brügge, B., 1991. Wind-produced water exchange between the deep basins of the Baltic Sea. Journal of Physical Oceanography 21, 373–384.
Kullenberg, G., 1981. Physical Oceanography. In: The Baltic Sea (Ed. Aarno Voipio), Elsevier Oceanography Series 30, p. 135–218.
Kysely, J., Domonkos, P., 2006. Recent increase in persistence of atmospheric circulation over Europe: Comparison with long-term variations since 1881. International Journal of Climatology 26, 461–483.
Lagemaa, P., Elken, J., Kõuts, T., 2011. Operational sea level forecasting in Estonia. Estonian Journal of Engineering, 17(4), 301–331.
Laine, A.O., Andersin, A.B., Leinio, S., Zuur, A.F., 2007. Stratification-induced hypoxia as a structuring factor of macrozoobenthos in the open Gulf of Finland (Baltic Sea). Journal of Sea Research 57, 65–77.
Lehmann, A., Krauss, W., Hinrichsen, H.H., 2002. Effects of remote and local atmospheric forcing on circulation and upwelling in the Baltic Sea. Tellus 54A, 299–319.
Lehmann, A., Getzlaff, K., Harlass, J., 2011. Detailed assessment of climate variability in the Baltic Sea area for the period 1958 to 2009. Climate Research 46, 185–196.
Lips, I., Lips, U., Liblik, T., 2009. Consequences of coastal upwelling events on physical and chemical patterns in the central Gulf of Finland (Baltic Sea). Continental Shelf Research 29, 1836–1847.
MacCready, P., Geyer, W.R., 2010. Advances in Estuarine Physics. Annual Review of Marine Science 2, 35–58.
Matthäus, W., 1984. Climatic and seasonal variability of oceanological parameters in the Baltic Sea. Beiträge zur Meereskunde, 51, 29–49.

Matthäus, W., Frank, H., 1992. Characteristics of major Baltic inflows – a statistical analysis. Continental Shelf Research 12, 1375–1400.

Meier, H.E.M., 2005. Modeling the age of Baltic Seawater masses: Quantification and steady state sensitivity experiments. Journal of Geophysical Research 110, doi:10.1029/2004JC002607

Meier, H.E.M., Feistel, R., Piechura, J., Arneborg, L., Burchard, H., Fiekas, V., Golenko, N., Kuzmina, N., Mohrholz, V., Nohr, C., Paka, V.T., Sellschopp, J., Stips, A., Zhurbas, V., 2006. Ventilation of the Baltic Sea deep water: A brief review of present knowledge from observations and models. Oceanologia 48,133–164.

Pärn, O., Haapala, J., 2011. Occurrence of synoptic flaw leads of sea ice in the Gulf of Finland. Boreal Environment Research 16, 71–78.

Pavelson, J., Laanemets, J., Kononen, K., Nõmmann, S., 1997. Quasi-permanent density front at the entrance to the Gulf of Finland: Response to wind forcing. Continental Shelf Research 17, 253–265.

Reyes-Hernandez, C., Valle-Levinson, A., 2010. Wind Modifications to Density-Driven Flows in Semienclosed, Rotating Basins. Journal of Physical Oceanography 40, 1473–1487.

Rodionov, S.N., 2004. A sequential algorithm for testing climate regime shifts. Geophysical Research Letters 31, doi:10.1029/2004GL019448

Scully, M.E., Friedrichs, C., Brubaker, J., 2005. Control of Estuarine Stratification and Mixing by Wind-induced Straining of the Estuarine Density Field. Estuaries 28 (3), 321–326.

Seifert T., Tauber F., Kayser B., 2001. A high resolution spherical grid topography of the Baltic Sea, Baltic Sea Science Congress, Stockholm 25–29 November 2001, Poster No. 147, Abstr. Vol., 2nd edn., [http://www.io-warnemuende.de/iowtopo].

Simpson, J.H., 1981. The shelf-sea fronts: implications of their existence and behaviour. Philosophical Transactions of the Royal Society London Series A 302, 531–546.

Simpson, J.H., Brown, J., Matthews, J., Allen, G., 1990. Tidal Straining, Density Currents, and Stirring in the Control of Estuarine Stratification. Estuaries 13 (2), 125–132.

Soomere, T., Keevallik, S., 2003. Directional and extreme wind properties in the Gulf of Finland. Proceedings of the Estonian Academy of Sciences. Engineering, 9, 2, 73-90

van Aken, H.M., 2008. Variability of the salinity in the western Wadden Sea on tidal to centennial time scales. Journal of Sea Research 59, 121–132.

Vermaat, J.E., Bouwer, L.M., 2009. Less ice on the Baltic reduces the extent of hypoxic bottom waters and sedimentary phosphorus release. Estuarine, Coastal and Shelf Science 82, 689–691.

Wang, B., Giddings, S.N., Fringer, O.B., Gross, E.S., Fong, D.A., Monismith, S.G., 2011. Modeling and understanding turbulent mixing in a macrotidal salt wedge estuary. Journal of Geophysical Research 116, doi:10.1029/2010JC006135

Zhang, Z., Leppäranta, M., 1995. Modeling the influence of ice on sea level variations in the Baltic Sea. Geophysica 31 (2), 31–45.

Zhurbas, V., Laanemets, J., Vahtera, E., 2008. Modeling of the mesoscale structure of coupled upwelling/downwelling events and the related input of nutrients to the upper mixed layer in the Gulf of Finland, Baltic Sea. Journal of Geophysical Research 113, doi:10.1029/2007JC004280

Figure captions

Figure 1. A map of the Baltic Sea (a) and close-up of the Gulf of Finland (b). Locations of the HELCOM monitoring station LL7/F3, Utö weather station and the main axis of the Gulf (red line) are shown. The depth contours are drawn from the gridded topography (Seifert et al. 2001) in meters.

Figure 2. Salinity values observed in the Gulf of Finland during winter (December-January) at station BMP F3 (dots), median and quartile values of all data (red lines) and profiles with collapsed stratification (black lines).

Figure 3. Temporal course of winter (December–January) bottom-to- surface density difference calculated from HELCOM monitoring data at location BMP F3 in 1976–2008.

Figure 4. Seasonal cycle of potential energy anomaly in the Gulf of Finland in a 15-km radius from the central station BMP F3. Data from 1990-2008.

Figure 5. Mean along-basin current and dimensional EOF modes (to yield unit standard deviation of time-dependent amplitude) along longitude 24.38°E for December and January during 2005-2009.

Figure 6. Vertical distribution of salinity on the main axis of the Gulf of Finland on 27 November (a) and 12 December 1999 (b) (isohalines at 0.5 intervals) and potential energy anomaly distribution (c) for 27 November (blue) and 12 December 1999 (red).

Figure 7. Temporal course of cumulative westerly-southwesterly component of wind stress (positive eastward) calculated from Utö weather station data (filled bars) for the period December–January in 1962–2007. Filled circles mark maximum cumulative wind stress within the period December–January for each winter. Black bold line shows the mean value using the Rodionov (2004) shift detection technique. Filled boxes on the *x*-axis show the winters of at least 50% ice cover appearance in December–January in the western Gulf of Finland.

Figure 8. Temporal course of wind mixing work over the period December–January (filled circles) calculated from Utö weather station data in 1962–2007. Black bold line shows the mean value using the Rodionov (2004) shift detection technique. Filled bars show wind mixing work over the period from the beginning of December until at least 50% ice cover in the western Gulf of Finland.

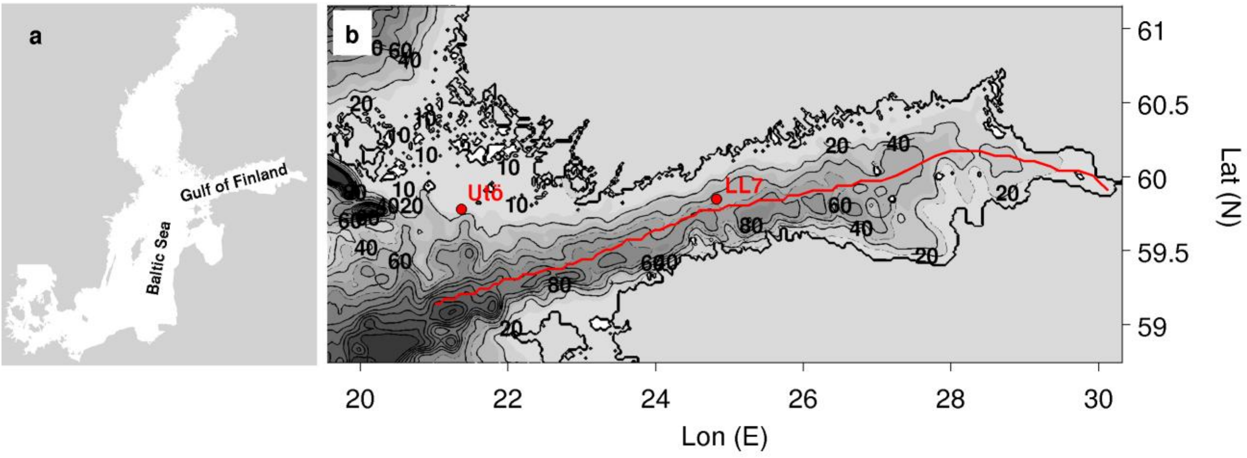

Figure 1. A map of the Baltic Sea (a) and close-up of the Gulf of Finland (b). Locations of the HELCOM monitoring station LL7/F3, Utö weather station and the main axis of the Gulf (red line) are shown. The depth contours are drawn from the gridded topography (Seifert et al. 2001) in meters.

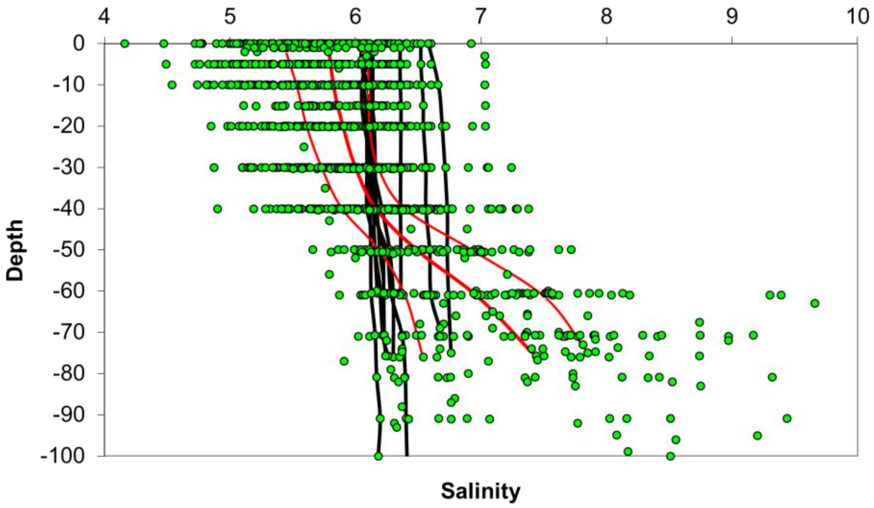

Figure 2. Salinity values observed in the Gulf of Finland during winter (December-January) at station BMP F3 (dots), median and quartile values of all data (red lines) and profiles with collapsed stratification (black lines).

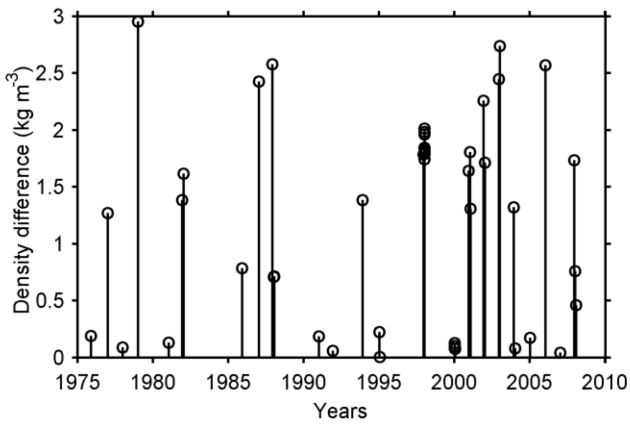

Figure 3. Temporal course of winter (December–January) bottom-to- surface density difference calculated from HELCOM monitoring data at location BMP F3 in 1976–2008.

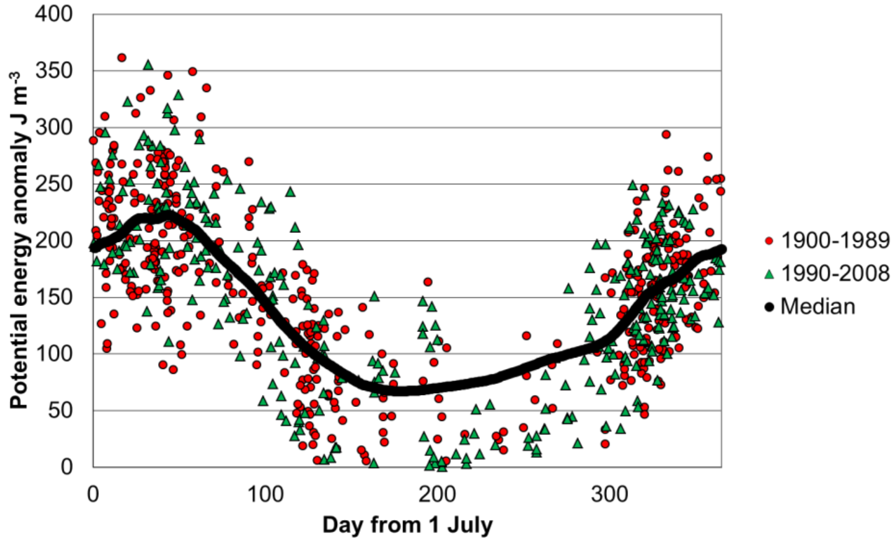

Figure 4. Seasonal cycle of potential energy anomaly in the Gulf of Finland in a 15-km radius from the central station BMP F3. Data from 1990-2008.

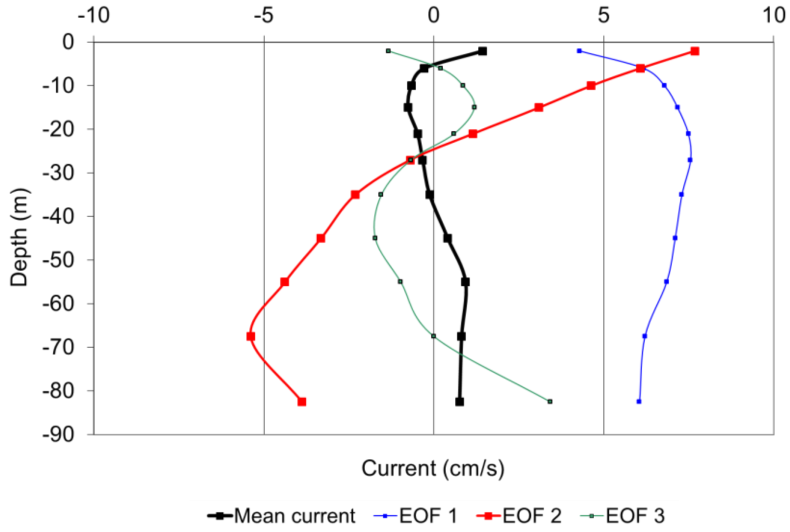

Figure 5. Mean along-basin current and dimensional EOF modes (to yield unit standard deviation of time-dependent amplitude) along longitude 24.38°E for December and January during 2005-2009.

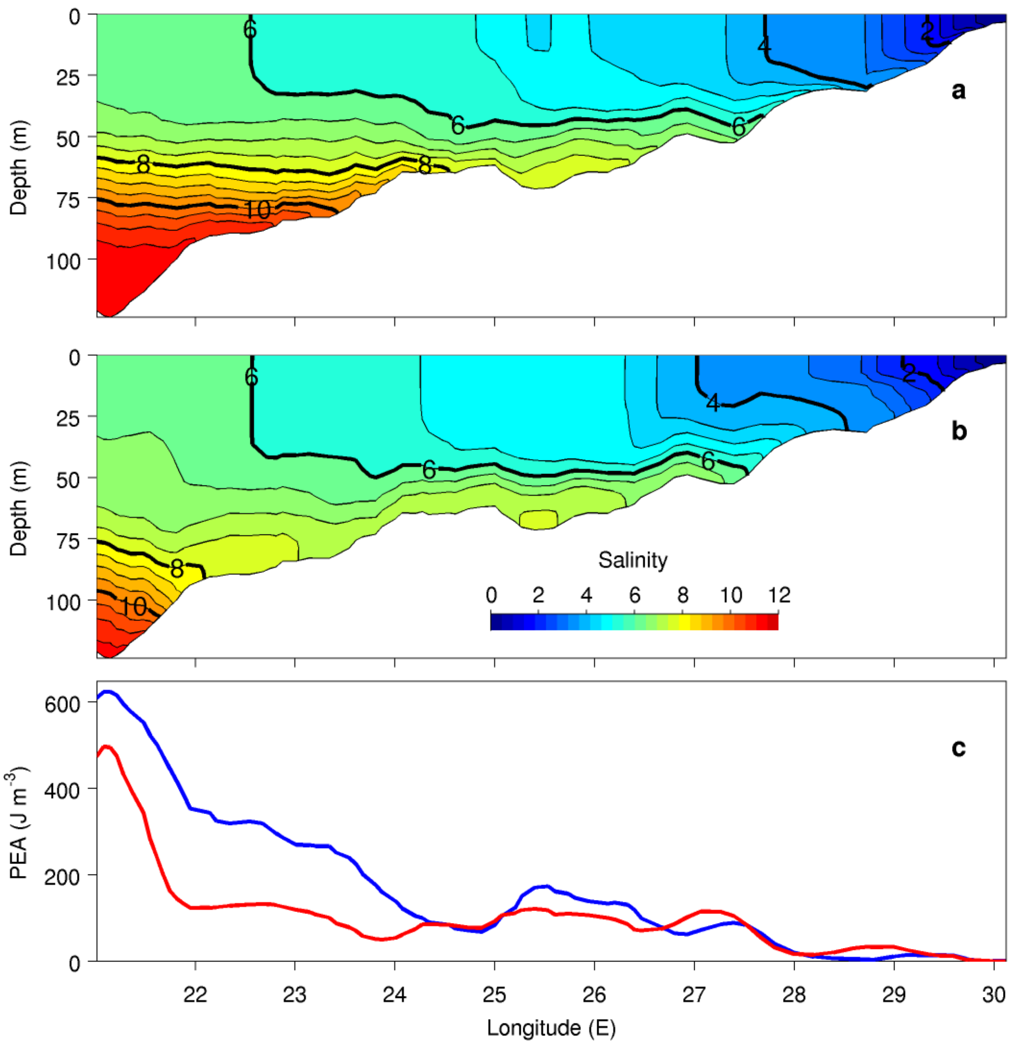

Figure 6. Vertical distribution of salinity on the main axis of the Gulf of Finland on 27 November (a) and 12 December 1999 (b) (isohalines at 0.5 intervals) and potential energy anomaly distribution (c) for 27 November (blue) and 12 December 1999 (red).

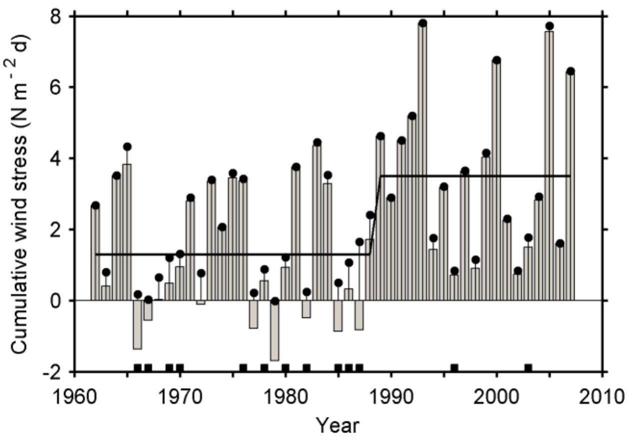

Figure 7. Temporal course of cumulative westerly-southwesterly component of wind stress (positive eastward) calculated from Utö weather station data (filled bars) for the period December–January in 1962–2007. Filled circles mark maximum cumulative wind stress within the period December–January for each winter. Black bold line shows the mean value using the Rodionov (2004) shift detection technique. Filled boxes on the *x*-axis show the winters of at least 50% ice cover appearance in December–January in the western Gulf of Finland.

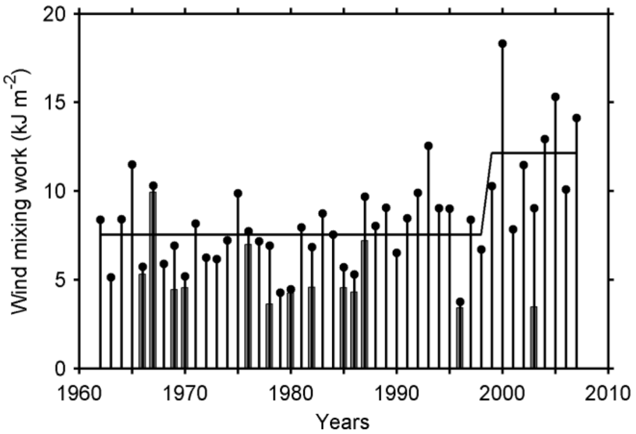

Figure 8. Temporal course of wind mixing work over the period December–January (filled circles) calculated from Utö weather station data in 1962–2007. Black bold line shows the mean value using the Rodionov (2004) shift detection technique. Filled bars show wind mixing work over the period from the beginning of December until at least 50% ice cover in the western Gulf of Finland.